LA-UR- 10-08132

Approved for public release; distribution is unlimited.

Title: The Dynamics of Unsteady Detonation with Diffusion

Author(s): Christopher M. Romick, University of Notre Dame
Tariq D. Aslam, LANL, WX-9
Joseph M. Powers, University of Notre Dame

Intended for: 49th AIAA Aerospace Sciences Meeting
Orlando, FL, USA
Jan 4-7, 2011

Los Alamos
NATIONAL LABORATORY
EST. 1943

The Dynamics of Unsteady Detonation with Diffusion

Christopher M. Romick *

Department of Aerospace and Mechanical Engineering, University of Notre Dame, Notre Dame, Indiana 46556

Tariq D. Aslam †

Dynamic and Energetic Materials Division, Los Alamos National Laboratory, Los Alamos, New Mexico 87545

Joseph M. Powers ‡

Department of Aerospace and Mechanical Engineering, University of Notre Dame, Notre Dame, Indiana 46556

The dynamics of one-dimensional detonations predicted by a one-step irreversible Arrhenius kinetic model with the inclusion of mass, momentum, and energy diffusion were investigated. A series of calculations in which activation energy is varied, holding the length scales of diffusion and reaction constant, was performed. As in the inviscid case, as the activation energy increases, the system goes through a period-doubling process and eventually undergoes a transition to chaos. Within the chaotic regime there exist regions of low frequency limit cycles. An approximation to Feigenbaum's constant, the rate at which bifurcation points converge, is obtained. The addition of diffusion significantly delays onset of instability and strongly influences the dynamics in the unstable regime.

I. Introduction

It is a common notion in detonation theory that the effects of diffusion can be segregated from the dynamics of both reaction and advection. There exists extensive literature (*cf.* Fedkiw *et al.*,[1] Oran *et al.*,[2] Hu *et al.*,[3] Wang *et al.*,[4] Walter and da Silva,[5] He and Karagozian,[6] Aslam and Powers,[7] or Tsuboi *et al.*[8]) which adopts the inviscid assumption. Using grid sizes around 10^{-6} m for their three-dimensional simulations of unsteady hydrogen-air detonations, Tsuboi *et al.* report wave dynamics that show strong sensitivity to the fineness of the grid. This suggests numerical diffusion is playing a significant role in determining the dynamics and that one should introduce grid-independent physical diffusion to properly capture the dynamics.

Powers and Paolucci[9] performed a spatial eigenvalue analysis on hydrogen-air and have shown for inviscid detonations that the length scales for a steady Chapman-Jouguet (CJ) detonation can span five orders of magnitude near equilibrium, with the smallest length scale for an ambient mixture at atmospheric pressure being 10^{-7} m and the largest being 10^{-2} m; away from equilibrium the breadth of scales can be even larger. These fine reaction scales are a manifestation of an averaged representation of the molecular collision model in which the fundamental length scale is the mean free path.[10] In order to have a mathematically verified prediction, this wide range of scales must be resolved, which poses a daunting task.

The choice of a one-step kinetic model induces a single reaction scale, in contrast to the multiple reaction scales of detailed kinetic models. This allows for the effects of the interplay between chemistry and transport phenomena on detonations be more easily studied. Such a model has been studied extensively; the stability and non-linear dynamics are well understood (*cf.* Lee and Stewart,[11] Bourlioux *et al.*,[12] Sharpe,[13] Kasimov and Stewart,[14] Ng *et al.*,[15] or Henrick *et al.* [16]) in the inviscid limit. Lee and Stewart developed a normal-mode approach to the linear stability of the idealized detonation to one-dimensional perturbations using a shooting method to find the unstable modes. Bourlioux *et al.* study the nonlinear development of instability. Kasimov and Stewart also applied a normal mode approach to the linear stability problem and performed a numerical analysis using a shock-tracking technique. Ng *et al.* developed a coarse bifurcation diagram

*Ph.D. Candidate, AIAA Member, cromick@nd.edu.

†Technical Staff Member, AIAA Member, aslam@lanl.gov.

‡Professor, AIAA Associate Fellow, powers@nd.edu.

showing how the oscillatory behavior became progressively more complex as activation energy increased. Henrick *et al.* developed a more detailed bifurcation diagram using a shock-fitting method in combination with a mapped WENO scheme.

The goal of this paper is to predict the effects of diffusion on the long-time dynamics of a detonation described by simple one-step kinetics. The plan of the paper is as follows. First the mathematical model is presented. This is followed by a description of the computational method. The model is used to predict the viscous analog of the period-doubling phenomena predicted in the inviscid limit by Sharpe, Ng *et al.*, and Henrick *et al.* The convergence of the period-doubling bifurcation points is shown to be in agreement with the general theory of Feigenbaum,[17,18] and diffusion is seen to have a generally stabilizing effect on detonation dynamics.

II. Mathematical Model

The model adopted here is the one-dimensional unsteady compressible reactive Navier-Stokes equations with one-step kinetics:

$$\frac{\partial \rho}{\partial t} + \frac{\partial}{\partial x}(\rho u) = 0, \tag{1}$$

$$\frac{\partial}{\partial t}(\rho u) + \frac{\partial}{\partial x}\left(\rho u^2 + P - \tau\right) = 0, \tag{2}$$

$$\frac{\partial}{\partial t}\left(\rho\left(e + \frac{u^2}{2}\right)\right) + \frac{\partial}{\partial x}\left(\rho u\left(e + \frac{u^2}{2}\right) + j^q + (P - \tau)\, u\right) = 0, \tag{3}$$

$$\frac{\partial}{\partial t}(\rho \lambda) + \frac{\partial}{\partial x}\left(\rho u \lambda + j_\lambda^m\right) = \rho r, \tag{4}$$

where the independent variables are time, t, and the spatial coordinate, x. In Eqs. (1-4), ρ is the mass density, u the particle velocity, P the pressure, τ the diffusive viscous stress, e the internal energy, j^q the diffusive heat flux, λ the reaction progress variable, j_λ^m the diffusive mass flux, and r the reaction rate. The equations were transformed to a frame of reference moving at a constant velocity, D. Applying this Galilean transformation, one recovers

$$\frac{\partial \rho}{\partial t} + \frac{\partial}{\partial x}(\rho\,(u - D)) = 0, \tag{5}$$

$$\frac{\partial}{\partial t}(\rho u) + \frac{\partial}{\partial x}(\rho u\,(u - D) + P - \tau) = 0, \tag{6}$$

$$\frac{\partial}{\partial t}\left(\rho\left(e + \frac{u^2}{2}\right)\right) + \frac{\partial}{\partial x}\left(\rho (u - D)\left(e + \frac{u^2}{2}\right) + j^q + (P - \tau)\, u\right) = 0, \tag{7}$$

$$\frac{\partial}{\partial t}(\rho \lambda) + \frac{\partial}{\partial x}\left(\rho\,(u - D)\,\lambda + j_\lambda^m\right) = \rho r. \tag{8}$$

The particle velocity, u, is still measured in the laboratory frame in Eqs. (5-8). The constitutive relations chosen for mass, momentum, and energy diffusion are

$$j_\lambda^m = -\rho \mathcal{D} \frac{\partial \lambda}{\partial x}, \tag{9}$$

$$\tau = \frac{4}{3}\mu \frac{\partial u}{\partial x}, \tag{10}$$

$$j^q = -k\frac{\partial T}{\partial x} + \rho \mathcal{D} q \frac{\partial \lambda}{\partial x}, \tag{11}$$

where Fick's Law for binary diffusion has been adopted as the model for diffusive mass flux, $\mathcal{D}$ is the mass diffusion coefficient, μ the dynamic viscosity, k the thermal conductivity, T the temperature, and q the heat release. A calorically perfect ideal gas model is adapted:

$$P = \rho R T, \tag{12a}$$

$$e = \frac{P}{\rho\,(\gamma - 1)} - q\lambda, \tag{12b}$$

where R is the gas constant, and γ is the ratio of specific heats. We choose the simple irreversible one-step reaction model to be $A \rightarrow B$, where A and B are the reactant and product, respectively; both have identical molecular masses and specific heats. In the undisturbed state, only A is present. The mass fractions of A and B are given by $1 - \lambda$, and λ, respectively. We take the reaction rate r to be given by the law of mass action with an Arrhenius rate sensitivity:

$$r = H(P - P_s) a (1 - \lambda) e^{-\frac{\tilde{E}_a}{P/\rho}}, \tag{13a}$$

Here a is the collision frequency factor, $\tilde{E}_a$ is the activation energy, and $H(P - P_s)$ is a Heaviside function which suppresses reaction when $P < P_s$, where P_s is a selected pressure. Also note the ambient pressure and density are taken to be P_o and ρ_o, respectively.

III. Computational Method

A point-wise method of lines approach is used. This method allows separate temporal and spatial discretizations and also allows for the inclusion of source terms. The advective terms were calculated using a combination of a fifth order WENO scheme and Lax-Friedrichs;[19] the diffusive terms are treated with sixth order central differences. As an aside, it is noted that a fifth order central differencing of the advection terms would work as well as a WENO discretization because our solutions contain no discontinuities. Temporal integration is accomplished using a third order Runge-Kutta scheme.

The exercise of demonstrating the harmony of the discrete solution with the foundational mathematics is known as verification.[20] The method of manufactured solutions[21] was used to verify the code. In this method, a solution form is assumed and source terms are added to the governing equations for the assumed solution form to satisfy them. A periodic form for the solution was assumed

$$\rho(x,t) = a_1 + b_1 \cos\left[\pi(x-t)\right], \tag{14}$$
$$u(x,t) = a_2 + b_2 \cos\left[\pi(x-t)\right], \tag{15}$$
$$p(x,t) = a_3 + b_3 \cos\left[\pi(x+t)\right], \tag{16}$$
$$\lambda(x,t) = a_4 + b_4 \cos\left[\pi(x+t)\right], \tag{17}$$

with a range $x \in [-1, 1]$. For the case presented here, $a_1 = a_2 = a_3 = a_4 = 1$ and $b_2 = b_3 = b_4 = 1/10, b_4 = 1$. The inital conditions being at $t = 0$. Fig. 1 shows asymptotic convergence of the solution to that assumed form. This indicates that the method is fifth order convergent in space. The y-axis is the sum of all variables L_1 errors normalized by the max value of the variable.

IV. Results

All calculations were performed in a single processor environment on an AMD 2.4 GHz processor with 512 kB cache. The program is initialized with the inviscid Zel'dovich-von Neumann-Döring (ZND) solution in a moving frame traveling at approximately the CJ speed. Each simulation is integrated in time for its long time behavior. For a calculation of 2.5 μs the computational time required was two days. Some calculations took as long as nine days to complete due to the need for longer integration times.

By selecting the diffusion coefficient, $\mathcal{D} = 10^{-4}\ m^2/s$, thermal conductivity, $k = 10^{-1}\ W/m/K$, and viscosity, $\mu = 10^{-4}\ Ns/m^2$ the Lewis, Le, Prandtl, Pr, and Schmidt, Sc numbers evaluated at the ambient density, $\rho_o = 1\ kg/m^3$, are unity. All of these parameters are within an order of magnitude of gases at a slightly elevated temperature. In the inviscid detonation, the activation energy controls the stability of the system; the rate constant merely introduces a length/time scale into the system, the half reaction length, $L_{1/2}$, (the distance between the inviscid shock and the location at which $\lambda = 1/2$). If the half reaction length is fixed, the effect of diffusion on the system can be studied. Using simple dimensional analysis of advection and diffusion parameters ($U = 1000\ m/s$ was chosen as a typical velocity scale) gives rise to an approximate length scale of mass diffusion, $\mathcal{D}/U = 10^{-7}\ m$, and likewise for momentum and energy diffusion $\mu/\rho_o/U = 10^{-7}\ m$, and $k/\rho_0/C_p/U = 10^{-7}\ m$. Since all the diffusion length scales are the same, let that scale be denoted as $L_\mu = 10^{-7}\ m$. The parameters in the governing equations, chosen in SI units are $P_o = 101325\ Pa$, $P_s = 200000\ Pa$, $\rho_o = 1\ kg/m^3$, $q = 5066250\ m^2/s^2$, $\gamma = 6/5$, and $\tilde{E}_a \in [2533125, 3232400]\ m^2/s^2$. With this heat release the D_{CJ} for the inviscid problem is,

$$D_{CJ} = \sqrt{\gamma \frac{P_o}{\rho_o} + \frac{q(\gamma^2-1)}{2}} + \sqrt{\frac{q(\gamma^2-1)}{2}} \approx 2167.56\ m/s. \tag{18}$$

To compare directly with previous work in the inviscid limit, the activation energies will be presented in dimensionless form, $E_a = \tilde{E_a}/\left(1.01325 \times 10^5\ m^2/s^2\right)$, thus $E_a \in [25, 32]$. Using these parameters allows for the interaction diffusion and reaction effects to be studied and the comparison with the inviscid results with the interaction of the two length scales of interest, reaction, $L_{1/2}$ and diffusion, L_μ.

A. Linearly stable and a limit cycle

In the inviscid case, linear stability analysis by Lee and Stewart revealed that for $E_a < 25.26$, the steady ZND wave is linearly stable and is otherwise linearly unstable. Henrick *et al.* numerically found the stability limit located at $E_a = 25.265 \pm 0.005$, which is in excellent agreement with prediction of the linear stability analysis. In examining a case well above that stability limit, $E_a = 26.647$, which Henrick *et al.*, found to relax to a period-1 limit cycle, it can be seen from Fig. 2 that in the presence of diffusion, there is no limit cycle behavior and the ZND viscous detonation predicted by steady theory is in fact stable. A steady limit cycle is realized by the system by increasing the activation energy to $E_a = 27.6339$, which is clearly shown in Fig. 3. The linear stability boundary for the diffusive case being studied was located at $E_a \approx 27.1404$.

B. Period-doubling and Feigenbaum's universal constant

As predicted by Sharpe and Ng *et al.* and shown in Henrick *et al.*, a period-doubling phenomena, similar to that predicted by the simple logistic map,[22,23] occurs at $E_a \approx 27.2$. The period-doubling effect predicted here is delayed, similarly to the initial linear instability. Fig. 4(a) shows the time history of the detonation pressure for the case $E = 29.6077$, which clearly shows in the long time limit two distinct relative maxima, $P \approx 6.256\ MPa$ and $P \approx 5.283\ MPa$; whereas for $E = 26.734$ only one relative maxima is present, $P \approx 4.867\ MPa$.

The activation energy at which the behavior switches from a period-1 to a period-2 solution is denoted as E_{a_1}. The other period-doubling bifurcation values, E_n, occur where the solution undergoes a transition from a period 2^{n-1} to a period 2^n. The transition from a linearly stable solution to a periodic solution is referred to as E_{a_0}. These bifurcation points are listed in Table 1; also listed are the bifurcation points of the inviscid problem studied by Henrick *et al.* and the approximations for the diffusive case studied here to Feigenbaum's Constant, δ_∞ :

$$\delta_\infty = \lim_{n\to\infty} \delta_n = \lim_{n\to\infty} \frac{E_n - E_{n-1}}{E_{n+1} - E_n}. \tag{19}$$

Feigenbaum predicted $\delta_\infty \approx 4.669201$. Table 1 shows three approximations to Feigenbaum's constant with the last approximation, $\delta_3 \approx 4.657$ being in good agreement with δ_∞.

Table 1. Numerically determined bifurcation points, comparison with inviscid, and approximations to Feigenbaum's Constant

	Inviscid	Diffusive	
n	E_{a_n}	E_{a_n}	δ_n
0	25.2650	27.1404	-
1	27.1875	29.3116	3.793
2	27.6850	29.8840	4.639
3	27.8017	30.0074	4.657
4	27.82675	30.0339	-

C. Bifurcation diagram, windows and chaos

A bifurcation diagram was constructed by sampling over 300 points with $E_a \in [25, 32]$, with the minimum spacing $\Delta E_a \approx 0.001$ occurring after the third bifurcation and a maximum spacing of $\Delta E_a \approx 0.1$ in the linearly stable region. For $E_a > E_{a_3}$ the solutions were integrated to $t = 10$ μs, and relative maxima in P were recorded for $t > 7$ μs. For those points below the third activation energy, solutions were only integrated to 2.5 μs, and relative maxima were recorded for $t > 1$ μs. The late time behavior of relative maxima in P versus activation energy is shown in Fig. 6(b). It shows the period-doubling bifurcations up to roughly $E_a \approx 30.0600$. Also of note are the regions in which a limit cycle exists with an odd number of periods. For example $E_a \approx 30.4$ a period-3 window exists; as E_a increases further, the period-3 behavior bifurcates to a period-6 behavior. It is likely that in the dense portions of the bifurcation diagram that the system is in the chaotic regime.

Fig. 4 gives several plots as activation energy is increased of P versus t. As E_a increases the system undergoes a bifurcation process, and chaos is achieved, which is qualitatively striking similar to the logistic map studied by Feigenbaum. Within the chaotic regime, there exist pockets of order. Periods of 5, 6, and 3 are found and are shown in (c), (e), and (f) respectively.

Table 2. Ranges of different periods

Period	E_a
Stable	< 27.1404
1	$[27.1404, 29.3116]$
2	$[29.3116, 29.8840]$
4	$[29.8840, 30.0074]$
8	$[30.0074, 30.0339]$
Chaotic	$[30.0600, 30.2591]$
5	$[30.2591, 30.2788]$
Chaotic	$[30.2788, 30.3578]$
5	$[30.3578, 30.3775]$
Chaotic	$[30.3775, 30.4071]$
3	$[30.4071, 30.4565]$
6	$[30.4565, 30.4959]$
Chaotic	$[30.4959, 30.8512]$
3	$[30.8512, 30.8611]$
6	$[30.8611, 30.9203]$
Chaotic	> 30.9203

D. Effect of diminishing diffusion

By increasing the reaction length scale, $L_{1/2}$, the relative effect of diffusion decreases. Fig. 5 shows solutions for $E_a = 27.634$, for the ratio of (a) $L_\mu/L_{1/2} = 1/5$, (b) $L_\mu/L_{1/2} = 1/10$, and (c) $L_\mu/L_{1/2} = 1/50$. The system undergoes a transition from a stable detonation to a limit cycle, and again to a period-2 limit cycle. It clearly shows an amplitude increase in the pulsations with (a) decaying to a $P_{max} \approx 4.213$ MPa, (b) having a relative maximum of $P_{max} \approx 4.799$ MPa and (c) having relative maxima of $P_{max} \approx 5.578$ MPa and $P_{max} \approx 5.895$. In addition to these behavioral changes, the frequency of the pulsations also decreases.

It can be clearly seen from Fig. 6 that the whole bifurcation diagram obtained by Henrick *et al.* using a shock-fitting algorithm in which the artificial viscosity is nearly negligible, occurs below the first period-doubling bifurcation of the diffusive case. Henrick *et al.* state that above $E_a \approx 30$ the secondary captured shocks may overtake the lead shock, which would negate precision of their shock fitting technique. In the diffusive case, the system is still in the period-doubling phase at $E_a \approx 30$. In the diffusive case there is no true discontinuity, thus the shock can not be predicted as in the inviscid limit. The trend that exists for the inviscid case also exists in the diffusive case. Ignoring diffusion can shift the system from a simple period-1 limit cycle to a fully chaotic regime.

V. Conclusion

Investigation of the one-step kinetic model of one-dimensional unsteady detonation with mass, momentum, and energy diffusion has shown that the dynamics of the system are significantly influenced in the region of instability. As in the inviscid limit, bifurcation and transition to chaos is predicted and shows similarities to the logistic map. The addition of the diffusion delays the onset of the instability. As physical diffusion is reduced, the behavior of the system trends towards the inviscid limit. The physical diffusion changes the behavior of the system dramatically and as it increases in comparison to the reaction length scale, the system becomes more stable. It is clear that if the dynamics of the denotation are to be captured correctly, that physical diffusion needs to be included in the model. It is likely that these results will extend to detailed kinetic systems. It is also likely that detonation cell pattern formation will be influenced by the magnitude of the physical diffusion.[24]

VI. Acknowledgements

The authors recognize the support of the National Aeronautics and Space Administration (NASA) under Grant No. NNX07AD10A and the National Science Foundation (NSF) under Grant No. CBET-0650843.

References

[1]Fedkiw, R. P., Merriman, B., and Osher, S., "High Accuracy Numerical Methods for Thermally Perfect Gas Flows with Chemistry," *Journal of Computational Physics*, Vol. 132, No. 2, 1997, pp. 175–190.

[2]Oran, E. S., Weber, J. W., Stefaniw, E. I., Lefebvre, M. H., and Anderson, J. D., "A Numerical Study of a Two-Dimensional $H_2 - O_2 - Ar$ Detonation Using a Detailed Chemical Reaction Model," *Combustion and Flame*, Vol. 113, No. 1-2, 1998, pp. 147–163.

[3]Hu, X. Y., Khoo, B. C., Zhang, D. L., and Jiang, Z. L., "The Cellular Structure of a Two-Dimensional $H_2/O_2/Ar$ Detonation Wave," *Combustion Theory and Modeling*, Vol. 8, No. 2, 2004, pp. 339–359.

[4]Wang, B., He, H., and Yu, S. T. J., "Direct Calculation of Wave Implosion for Detonation Initiation," *AIAA Journal*, Vol. 43, No. 10, 2005, pp. 2157–2169.

[5]Walter, M. A. T. and da Silva, L. F. F., "Numerical Study of Detonation Stabilization by Finite Length Wedges," *AIAA Journal*, Vol. 44, No. 2, 2006, pp. 353–361.

[6]He, X. and Karagozian, A. R., "Pulse-Detonation-Engine Simulations with Alternative Geometries and Reaction Kinetics," *Journal of Propulsion and Power*, Vol. 22, No. 4, 2006, pp. 852–861.

[7]Aslam, T. D. and Powers, J. M., "The Dynamics of Unsteady Detonation in Ozone," *47th AIAA Aerospace Science Meeting and Exhibit*, AIAA, 2009, AIAA 2009-0632.

[8]Tsuboi, N., Eto, K., and Hayashi, A. K., "Detailed Structure of Spinning Detonation in a Circular Tube," *Combustion and Flame*, Vol. 149, No. 1-2, 2007, pp. 144–161.

[9]Powers, J. M. and Paolucci, S., "Accurate Spatial Resolution Estimates for Reactive Supersonic Flow with Detailed Chemistry," *AIAA Journal*, Vol. 43, No. 5, 2005, pp. 1088–1099.

[10]Al-Khateeb, A. N., Powers, J. M., and Paolucci, S., "On the Necessary Grid Resolution for Verified Calculation of Premixed Laminar Flames," *Communications in Computational Physics*, Vol. 8, No. 2, 2010, pp. 304–326.

[11]Lee, H. I. and Stewart, D. S., "Calculation of Linear Detonation Instability: One-dimensional Instability of Planar Detonations," *Journal of Fluid Mechanics*, Vol. 216, 1990, pp. 103–132.

[12]Bourlioux, A., Majda, A. J., and Roytburds, V., "Theoretical and Numerical Structure for Unstable One-Dimensional Detonations," *SIAM Journal on Applied Mathematics*, Vol. 51, No. 2, 1991, pp. 303–343.

[13]Sharpe, G. J., "Linear stability of idealized detonations," *Proceedings of the Royal Society of London Series A Mathematical Physical and Engineering Sciences*, Vol. 453, No. 1967, 1997, pp. 2603–2625.

[14]Kasimov, A. R. and Stewart, D. S., "On the Dynamics of Self-Sustained One-Dimensional Detonations: A Numerical Study in the Shock-Attached Frame," *Physics of Fluids*, Vol. 16, No. 10, 2004, pp. 3566–3578.

[15]Ng, H. D., Higgins, A. J., Kiyanda, C. B., Radulescu, M. I., Lee, J. H. S., Bates, K. R., and Nikiforakis, N., "Nonlinear dynamics and chaos analysis of one-dimensional pulsating detonations," *Combustion Theory and Modeling*, Vol. 9, No. 1, 2005, pp. 159–170.

[16]Henrick, A. K., Aslam, T. D., and Powers, J. M., "Simulations of Pulsating One-Dimensional Detonations with True Fifth Order Accuracy," *Journal of Computational Physics*, Vol. 213, No. 1, 2006, pp. 311–329.

[17]Feigenbaum, M. J., "Quantitative Universality for a Class of Non-linear Transformations," *Journal of Statistical Physics*, Vol. 19, No. 1, 1978, pp. 25–52.

[18]Feigenbaum, M. J., "The Universal Metric Properties of Nonlinear Transformations," *Journal of Statistical Physics*, Vol. 21, No. 6, 1978, pp. 669–706.

[19]Xu, S., Aslam, T. A., and Stewart, D. S., "High Resolution Numerical Simulation of Ideal and Non-ideal Compressible Reacting Flows with Embedded Internal Boundaries," *Combustion Theory and Modeling*, Vol. 1, 1997, pp. 113–142.

[20]Oberkampf, W. L. and Trucano, T. G., "Verification and Validation in Computational Fluid Dynamics," *Progress in Aerospace Sciences*, Vol. 38, 2002, pp. 209–272.

[21]Roache, P. J., "Code Verification by the Method of Manufactured Solutions," *Journal of Fluids Engineering*, Vol. 124, No. 1, 2002, pp. 4–10.

[22]May, R. M., "Simple Mathematical Models with Very Complicated Dynamics," *Nature*, Vol. 261, 1976, pp. 459–467.

[23]Drazin, P. G., *Nonlinear Systems*, Cambridge University Press, 1992.

[24]Powers, J. M., "Review of Multiscale Modeling of Detonation," *Journal of Propulsion and Power*, Vol. 22, No. 6, 2006, pp. 1217–1229.

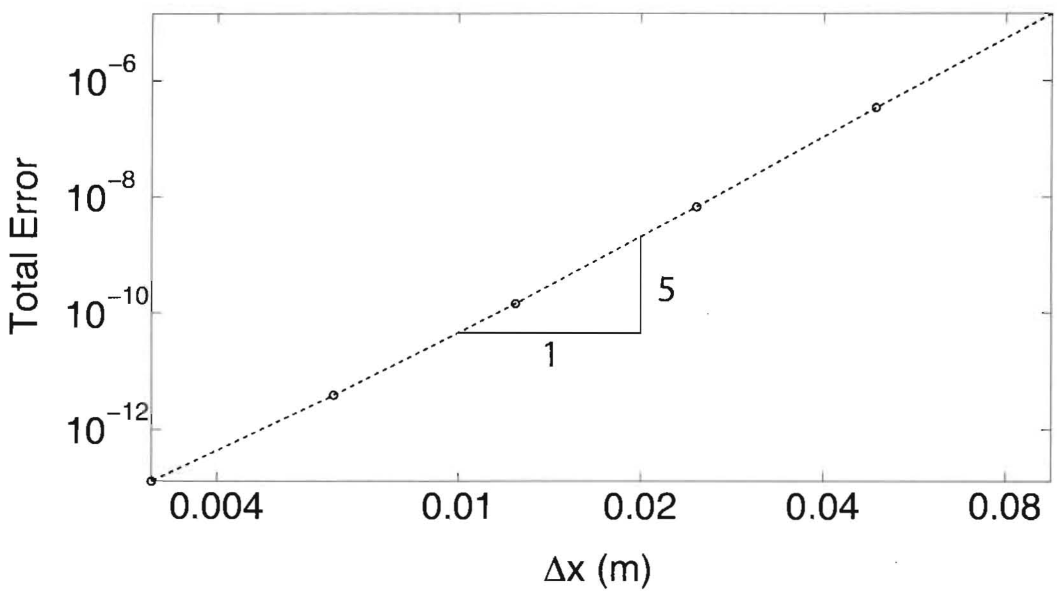

Figure 1. The normalized L_1 error versus Δx for a manufactured solution.

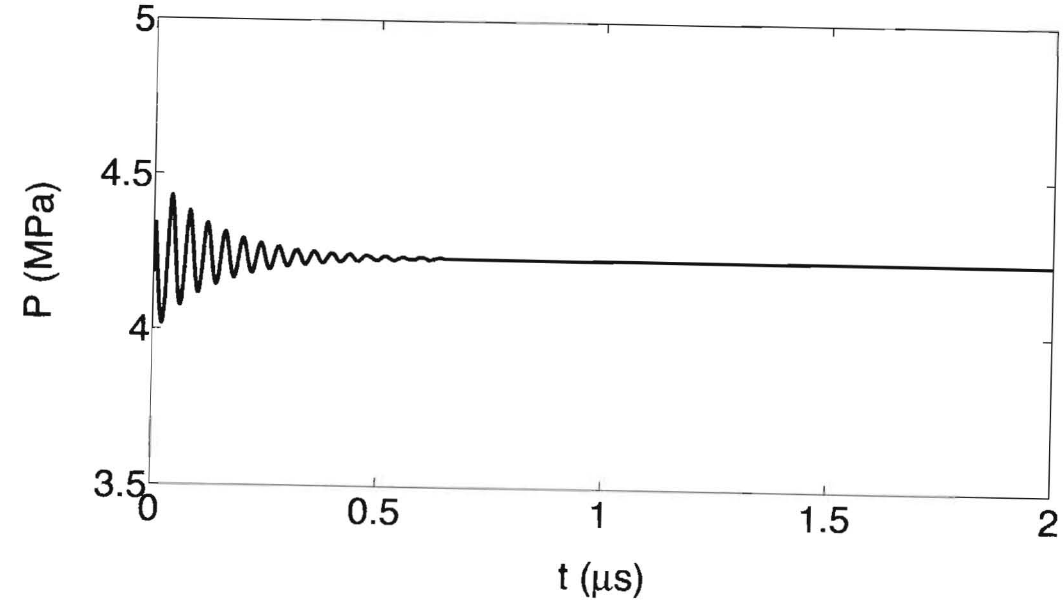

Figure 2. **Numerically generated detonation pressure,** P_{max} **versus** t, $E_a = 26.647$, $L_{1/2}/L_\mu = 1/10$, **stable.**

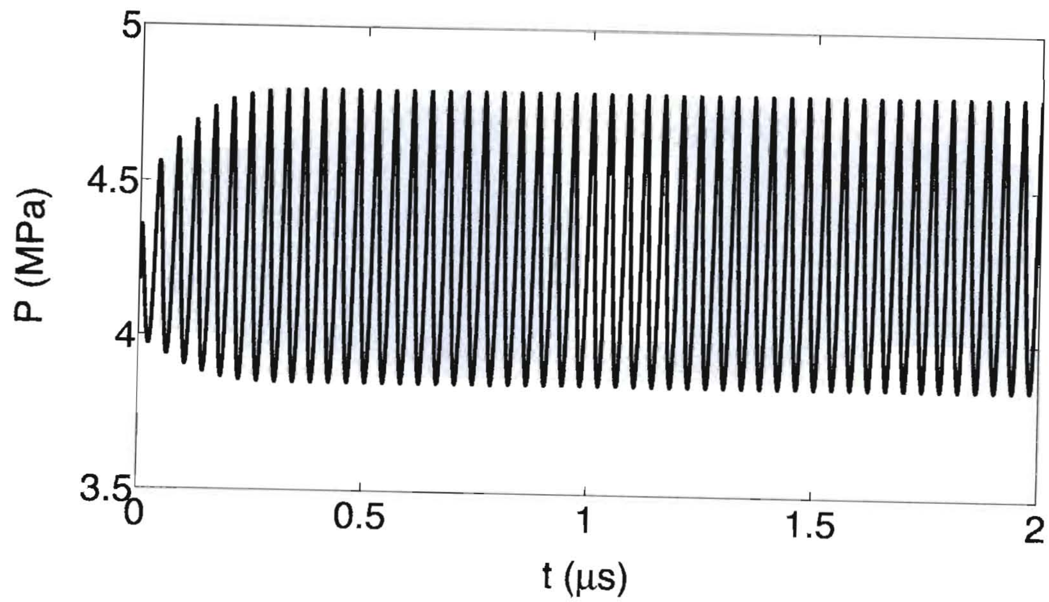

Figure 3. **Numerically generated detonation pressure,** P_{max} **versus** t, $E_a = 27.6339$, $L_{1/2}/L_\mu = 1/10$, **period-1 oscillations shown.**

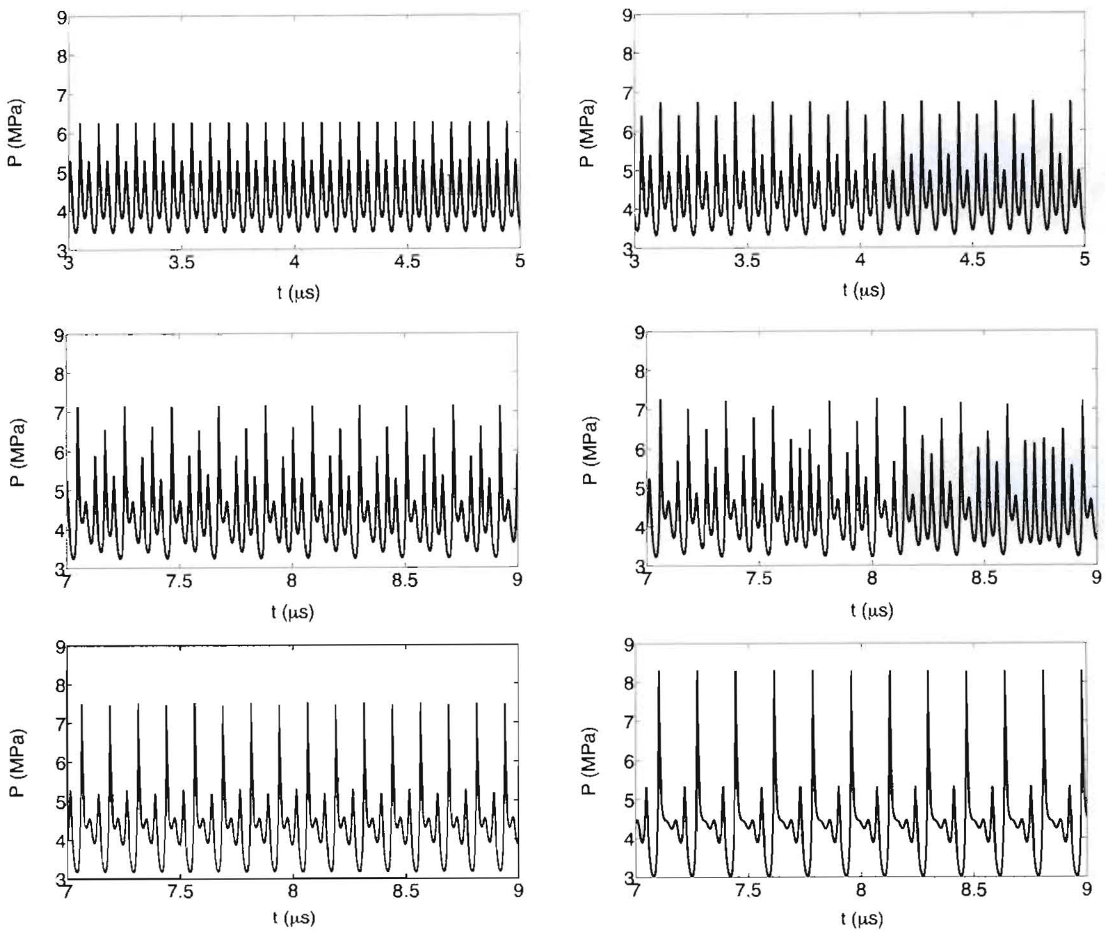

Figure 4. Numerically generated detonation pressure, P_{max} versus t :(a) E_a = 29.6077, period-2, (b) E_a = 30.0025, period-4, (c) E_a = 30.2689, period-5, (d) E_a = 30.3578, chaotic, (e) E_a = 30.4762, period-6, (f) E_a = 30.8512, period-3.

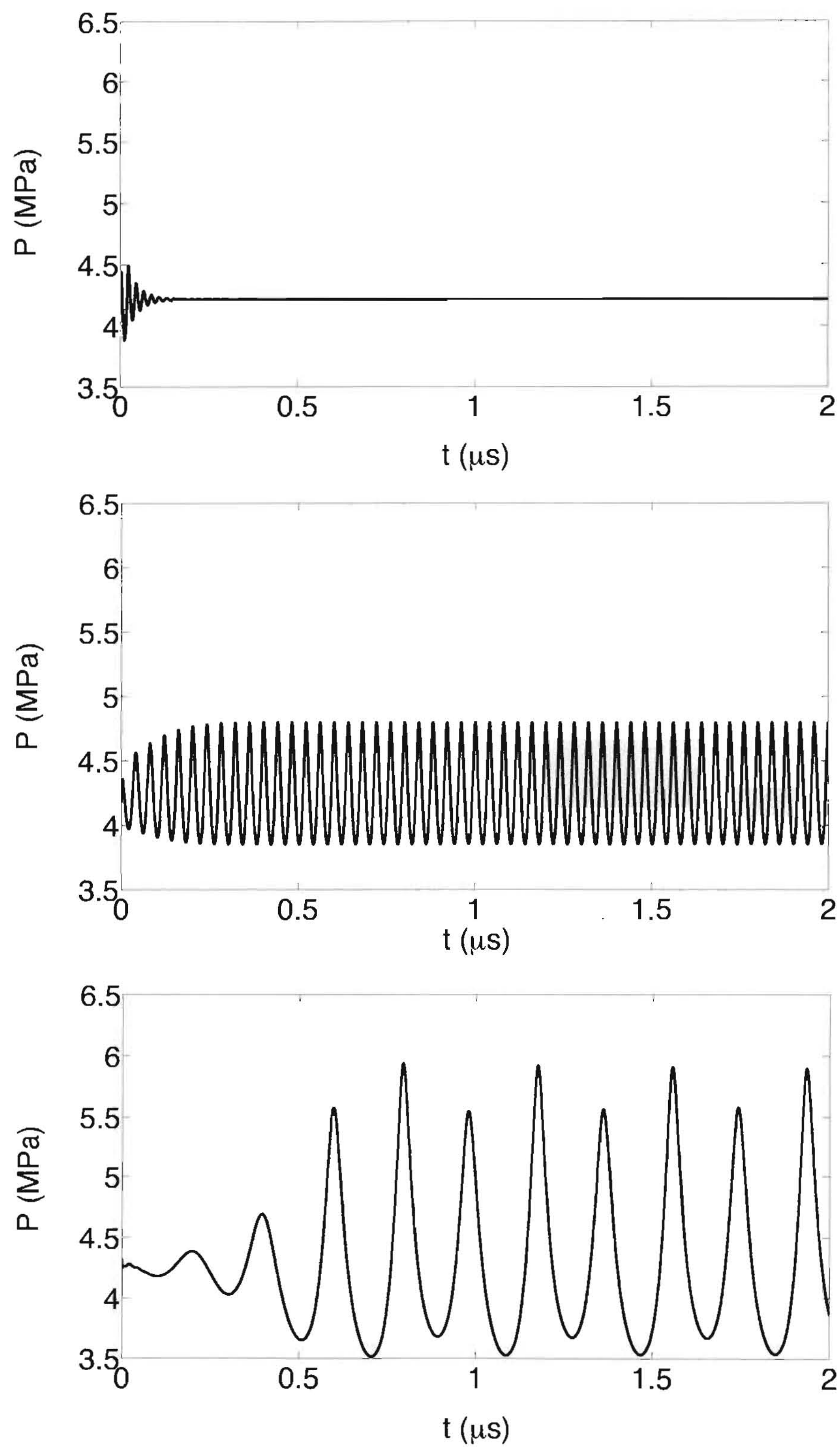

Figure 5. **Numerically generated detonation pressure, P_{max} versus t for $E_a = 27.6339$ and (a)$L_\mu/L_{1/2} = 1/5$, stable and (b)$L_\mu/L_{1/2} = 1/10$, period-1, and (c)$L_\mu/L_{1/2} = 1/50$, period-2.**

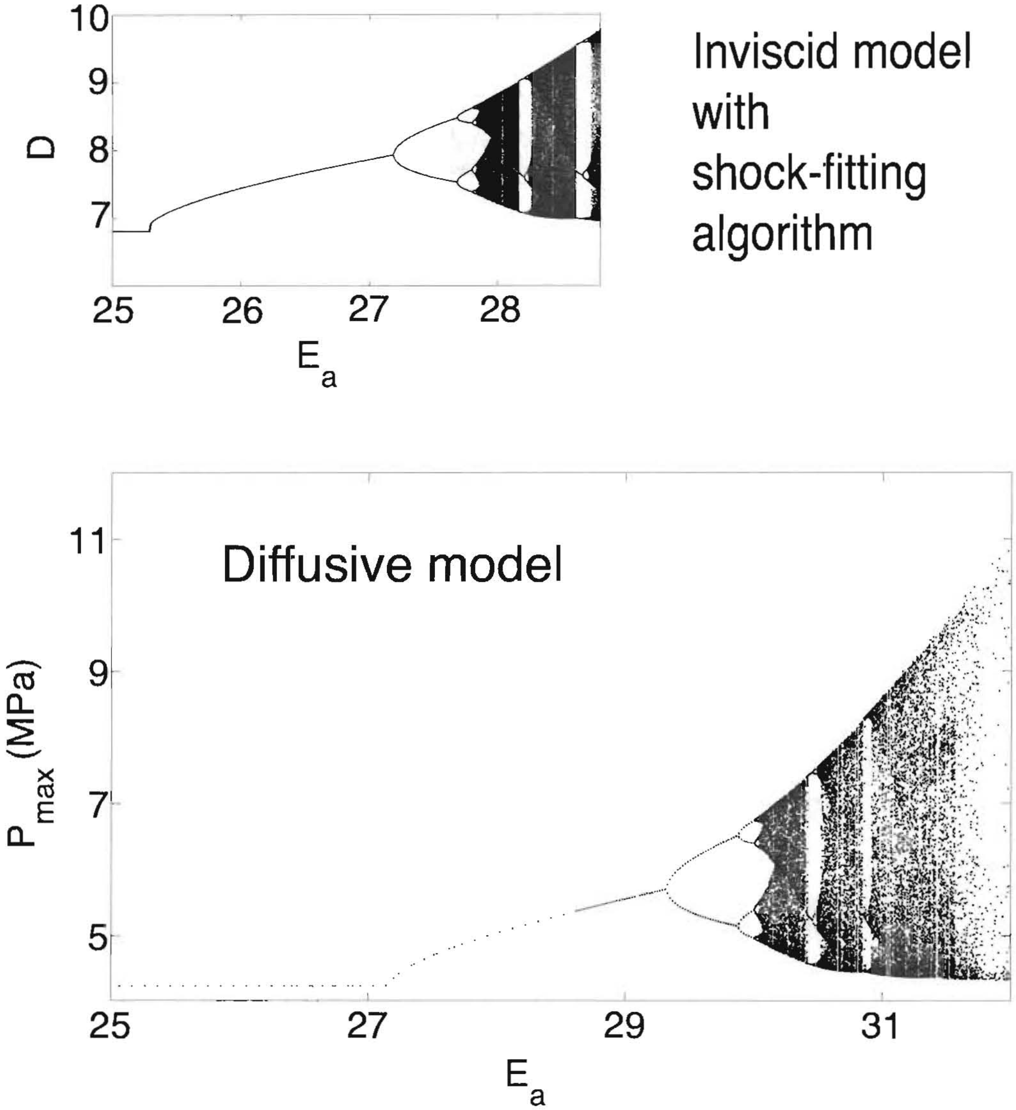

Figure 6. Comparison of numerically generated bifurcation diagrams, inviscid diagram by Henrick *et al.*, and $L_\mu/L_{1/2} = 1/10$.